Interaction of haptoglobin with hemoglobin octamers based on the mutation αAsn78Cys or βGly83Cys

Thomas Brillet[1], Michael C. Marden[1*], Joanne I. Yeh[2], Tong-Jian Shen[3], Nancy T. Ho[3], Regina Kettering[2], Shoucheng Du[2], Corinne Vasseur[1], Elisa Domingues-Hamdi[1], Chien Ho[3], Véronique Baudin-Creuza[1]

[1]Inserm U779, Université Paris XI et VII, CHU Bicêtre, Le Kremlin-Bicêtre, France
[2]Department of Structural Biology, School of Medicine, University of Pittsburgh, Pittsburgh, USA
[3]Department of Biological Sciences, Carnegie Mellon University, Pittsburgh, USA
Email: *michael.marden@inserm. fr

ABSTRACT

Octameric hemoglobins have been developed by the introduction of surface cysteines in either the alpha or beta chain. Originally designed as a blood substitute, we report here the structure and ligand binding function; in addition the interaction with haptoglobin was studied. The recombinant Hbs (rHbs) with mutations alpha Asn78Cys or beta Gly83Cys spontaneously form octamers under conditions where the cysteines are oxidized. Oxygen binding curves and CO kinetic studies indicate a correct allosteric transition of the tetramers within the octamer. Crystallographic studies of the two rHbs show two disulfide bonds per octamer. Reducing agents may provoke dissociation to tetramers, but the octamers are stable when mixed with fresh human plasma, indicating that the reduction by plasma is slower than the oxidation by the dissolved oxygen, consistent with an enhanced stability. The octameric rHbs were also mixed with a solution of haptoglobin (Hp), which binds the dimers of Hb: there was little interaction for incubation times of 15 min; however, on longer timescales a complex was formed. Dynamic light scattering was used to follow the interaction of Hp with the alpha Asn78Cys octamer during 24 hours; a transition from a simple complex of 15 nm to a final size of 60 nm was observed. The results indicate a specific orientation of the αβ dimers may be of importance for the binding to haptoglobin.

Keywords: Octamers; Hemoglobin; Haptoglobin; Allosteric Transition; Crystallography

1. INTRODUCTION

The classical human adult hemoglobin (HbA) is a hetero-

*Corresponding author.

tetramer ($\alpha_2\beta_2$), whose main function is the transport of oxygen from the lungs to tissues. The crucial role of intra and inter-subunits contacts in the allosteric ligand binding function of human Hb has been well studied both experimentally and theoretically [1]. Different Hb molecules or vectors have been designed as blood substitutes, with the intention to increase the size of the transporter to ensure a longer circulation time [2-5]. Higher oligomeric forms are possible via surface cysteine reactions. In HbA, 6 cysteine residues are present, one in each α-subunit at position 104 and two in each β-subunit at positions 93 and 112, but none are involved in disulfide bridges. Twenty-two natural Hb variants have been reported with a point mutation resulting in a cysteine residue [6], fourteen in the β-chain and eight in the α-chain.

Among these variants, Hb Ta-Li [$\alpha_2\beta_2$Gly83→Cys] has been reported to polymerize after lysis of the red blood cells, probably due to oxidation of the cysteines which are normally in the reducing environment of the cytoplasm of the red blood cell [7]. We have previously reported certain properties of recombinant Hb (rHb) (βGly83Cys) which form octamers via the cysteine on the protein surface [8]. The residue βG83 (EF7), between helices E and F, provides a surface accessible site to join tetramers via a disulfide bond. We have also produced the rHb (αAsn78Cys) at the analogous residue (EF7) on the α-chains. In this study, we report initial crystallographic data of these octameric Hbs; a detailed description of our X-ray crystallographic results will be published elsewhere.

We also investigate the functional properties and the disulfide bond stability of rHb (αAsn78Cys) in comparison to those observed with rHb (βGly83Cys), and the interaction of these octamers with haptoglobin (Hp). Hp is a plasma glycoprotein which binds Hb dimers [9] and participates in the elimination of Hb from circulation. Note that the octamers consist of two tetramers that are still free to individually separate into dimers. The rare

event of separation of both tetramers into dimers would expose the components $\alpha\beta$(S-S)$\beta\alpha$ or the symmetric analogue $\beta\alpha$(S-S)$\alpha\beta$. Capture of such species by Hp is thus of interest. During intravascular hemolysis, Hb released into plasma is captured by Hp; the Hp-(Hb dimer) complex is then recognized by the CD163 macrophage scavenger receptor which mediates the internalization of the Hb-Hp complexes by macrophages [10]. A soluble form of the CD163 receptor in the plasma has also been described [11]. Human Hp consists of two heavy (H or β) chains which are connected by two light (L or α) chains via a disulfide bridge between the L chains. To avoid confusion with the Hb chains, we will use the L and H notation. The L-chains recognize the dimer of Hb to form a Hp-(Hb dimer) complex. The Hp (HLLH) molecule defines the Hp(1-1) phenotype. A human variant with a longer L-chain is also present and leads to multimeric Hps designed Hp(2-2) and Hp(2-1) [12]. These different multimeric Hps also bind Hb dimers. We have made a particular study of the interaction between the rHb (αAsn78Cys) and Hp(1-1) by measuring particle size versus time. The difference in reaction of Hp with these new species could provide information on the poorly understood interaction of Hp with dimers.

2. MATERIALS AND METHODS

2.1. Preparation of Mutant rHbs

The mutated Hbs were produced in JM 109 strains of *Escherichia coli* using the expression plasmid pHE2 or pHE7 containing human α-, β-globin cDNAs and an *E. coli* methionine aminopeptidase cDNA [13,14], after introduction of the mutation αAsn78Cys or βGly83Cys by site-directed mutagenesis. After isolation and purification of the rHbs, the oligomeric and tetrameric fractions were then separated by size exclusion chromatography (SEC) on a Superose^{TM} 12 HR 10/300 GL column (GE Healthcare Lifescience, Uppsala, Sweden) equilibrated at 25°C in PBS [8].

2.2. Test of the Octamer to Tetramer Dissociation in Fresh Plasma

The αAsn78Cys or βGly83Cys octamers were mixed with fresh human plasma at a final concentration of 14 mg/ml at 37°C. At different times, an aliquot was withdrawn, centrifuged and analyzed by SEC on Superose^{TM} 12 HR 10/300 GL column.

2.3. Test of the Interaction with Human Hp

Reaction with human Hp (Hp1-1, Sigma Aldrich, Saint Quentin Fallavier, France) was made at room temperature in PBS containing Hp at 0.5 mg/ml and either α or β octamers at 0.46 mg/ml. At different times of incubation,

the presence of different species was analyzed by SEC on a Superose^{TM} 12 HR 10/300 GL column. In parallel, control reactions were made with HbA and diaspirin cross-linked hemoglobin (DCL-Hb) tetramer, at 0.33 mg/ml. The size of the different species formed was measured by dynamic light scattering (DLS) with a Nano ZS (Malvern Instruments Ltd, Worcestershire, UK). Measurements were performed at 25°C in PBS at least 5 times on each sample and the average was taken for the hydrodynamic radius.

2.4. Ligand Rebinding Kinetics

The bimolecular recombination kinetics were measured at 37°C, after flash photolysis using 10-ns YAG laser pulses (CFR 200, Quantel, Les Ulis, France) at 532 nm, with variable pulse energy to 160 mJ. Samples at 5 to 10 μM on a heme basis were in 4×10 mm quartz cuvettes with observation at 436 nm [15,16]. In a first measurement, the laser energy was reduced by half successively from 100% to 12.5% (to lower the fraction of the heme-CO photo-dissociation) to study the allosteric behavior of the α and β octamers. In a second measurement, inositol hexaphosphate (IHP), an analogue of the 2,3 diphosphoglycerate (DPG) effector, was added at a final concentration of 1 mM to enhance the fraction of the low affinity (T) state. Samples were equilibrated under 10% or 100% CO. Measurements were made before and just after addition of dithionite, which was added to ensure full iron reduction and to remove any traces of O_2. Dithionite also reduces the cysteine residues and may thus break the disulfide bonds; this occurs after about 30 min of incubation, (data not shown), so it was added just before (less than 1 min) the beginning of the experiments.

2.5. Oxygen-Binding Measurements

The experiments were carried out using a Hemox Analyzer (TCS Medical Products, Huntington, Valley, PA). As previously described, the experiments were run at 29°C as a function of pH in 0.1 M sodium phosphate buffer and contained 0.1 mM Hb (on a heme basis) [13, 14,17]. The P_{50} values (in mmHg) and the n_{50} values are given with an accuracy of ± 10%.

2.6. Crystallization and Structure Determination

Crystals were grown at 14°C by combining 1 μl of Hb protein stock solution (40 mg/ml in 10 mM sodium phosphate buffer, pH 7.0) with 1 μl crystallization solutions in vapor-diffusion sitting-drop trays. Plate-like crystals of β octamers were obtained from 20% PEG 3500, 0.1 M Tris-HCl pH 9.0, 0.25 M sodium bromide, and 0.4 M calcium phosphate, indexed in a triclinic (P1) space group, diffracting to a resolution of 2.65 Å. Crystals of α

octamers were grown from 0.35 M lithium sulphate, 0.15 M cadmium chloride, 0.1 M Tris-HCl pH 8.5, 25.5% PEG 8000, and 15% sorbitol, indexed in an orthorhombic ($P2_12_12_1$) space group, diffracting to a resolution of 2.25 Å. For the β octamers, 180° of data were collected at the GM/CA 23-ID beamline and for the α octameric crystals, 180° of data were collected at the SER-CAT 22-BM-ID beamlines (Argonne National Labs).

Data were processed, scaled, and analyzed using HKL-2000, d*TREK, and PHENIX [18-21] and molecular replacement trials using a dimeric model of CO-bound Hb (PDB accession number 1BBB) [22] were done in Phaser [23]. All structures were refined using iterative cycles of energy minimization in CNS, restrained refinement in Refmac5 [24], and least-squares refinement in PHENIX [20], monitoring R_{work} and R_{free} [25] throughout model building and fitting cycles. Prior to addition of solvent molecules, R_{work}/R_{free} for the βG83C and αN78C structures were 18.7/27.3% and 20.7/25.0%, respectively; data statistics are shown in **Table 1**. The structures were checked using the validation tools in Coot [26], SFcheck [27], and Procheck [28], all part of the CCP4 suite [29].

3. RESULTS

3.1. Crystal Structures

The X-ray crystallographic structures of rHb (βGly83Cys) and rHb (αAsn78Cys) clearly show the octameric states for these mutated Hb proteins (**Figure 1**). There are two disulfide bonds per octamer, consistent with the symmetry of the tetramers. The individual tetramers maintain

Table 1. Crystallographic data processing statistics.

	αAsn78Cys	βGly83Cys
Total Reflections	94397	133284
Unique Reflections	56819	72530
Resolution (Å)	50 - 2.25	50 - 2.65
Space group	$P2_12_12_1$	P1
Unit cell (Å)		
a	55.3	83.8
b	114.0	83.1
c	207.6	103.9
α	90	68.2
β	90	85.6
γ	90	90.4
Completeness (%)	90.4 (64.9)[a]	98.5 (95.9)
I/σ(I)	9.46 (1.9)	5.85 (1.95)
R_{sym}[b] (%)	12.5 (45.9)	8.0 (45.4)

[a]Numbers in parentheses are values for the highest resolution shell; [b]$R_{sym} = \Sigma_h\Sigma_i|I(h,i) - <I(h)>|/\Sigma_h\Sigma_i I(h,i)$ where $I(h,i)$ is the intensity values of the ith measurement of h and $<I(h)>$ is the corresponding mean values of $I(h)$ for all i measurements.

the known conformation except in certain inter-helical segments. As shown in **Figure 1(a)**, a large central cavity is formed between the two tetramers. A view of the "docking" site, as seen by an approaching tetramer, is presented in **Figure 1(b)**, showing that the cysteines are near the central cavity of the Hb tetramer. Note that the rHb (βGly83Cys) and rHb (αAsn78Cys) will be referred as β octamer and α octamer, respectively in the work.

3.2. CO Rebinding Kinetics

Reflecting the allosteric behavior, Hb tetramers exists in two affinity states, a low-affinity T-state having the quaternary structure of deoxygenated Hb, and a high-affinity R-state characteristic of fully liganded Hb. Under normal conditions, Hb with three or four ligands has the R-state affinity, while Hb with zero or one ligand is in the T-state; the allosteric transition occurs typically at the doubly liganded level. At equilibrium, the partially liganded forms are not highly populated, due to the all or nothing effect of the allosteric transition. However, higher populations can be generated by photodissociation of the ligands. As for HbA, both the α and β octamers display the typical biphasic kinetics of recombination of CO after flash photolysis.

The kinetics for the β octamers have been previously described [8]; the kinetics for the α octamer are shown in **Figure 2(a)**. At full laser energy, there is a bimolecular signal of about 50%, meaning half of the heme-CO molecules were dissociated and the CO moves out of the heme pocket to the solvent. In this case, we observe a significant T-state population in the kinetics. By lowering the laser energy, less heme-CO molecules were dissociated and less of the slow T-like phase is observed (**Figure 2(a)**). At sufficiently low photolysis levels, the main photoproduct is the triply liganded form (considering the tetramers) and a nearly pure R-state form can be observed.

The R-state kinetics were obtained at photo-dissociation levels of typically 10% of the hemes. The initial rate of recombination of CO of the R state is different for HbA and the octamers. HbA has a rate of recombination of CO of 9 $\mu M^{-1} \cdot s^{-1}$, the β octamer 6.5 $\mu M^{-1} \cdot s^{-1}$ and the α octamer 5 $\mu M^{-1} \cdot s^{-1}$ (**Figure 2**). This could be explained by a heme pocket deformation due to the constraints of the disulfide bonds. In the case of the α octamer, equilibrated under an atmosphere of 10% CO at 37°C without effectors, one observes 58% of the slow T-like phase (**Figure 2(a)**) at full laser power, where about half of the hemes are without ligand at the beginning of the bimolecular phase. Under the same conditions of high laser level, the β octamer shows 32% of the slow phase while the reference HbA shows an intermediate value of 40%. At low photodissociation levels of about 10% of the hemes, the relative amount of slow phase was 8%, 4%, and 2.5% for

(a)   (b)
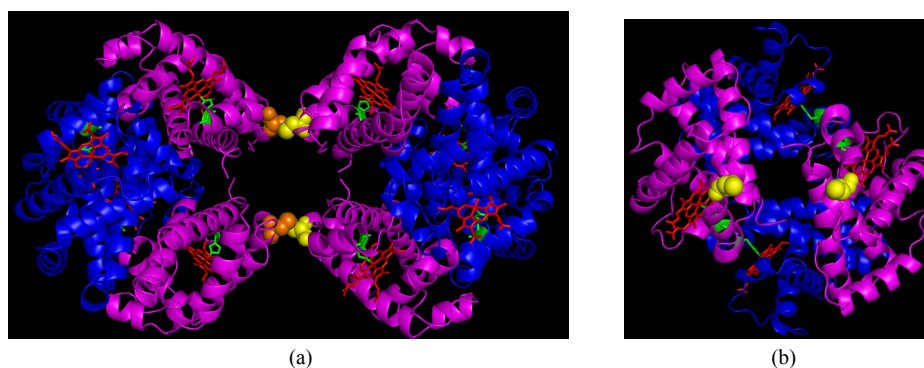
Figure 1. Crystallographic structure of octameric rHb βG83C. The cysteines, introduced at position β83 are shown in yellow on one tetramer and orange on the other, with β-chains in magenta and α-chains in blue. (a) Full octamer; by symmetry, two disulfide bonds per octamer are formed; (b) "Docking" view of one tetramer, as seen from an approaching tetramer.

(a)   (b)   (c)
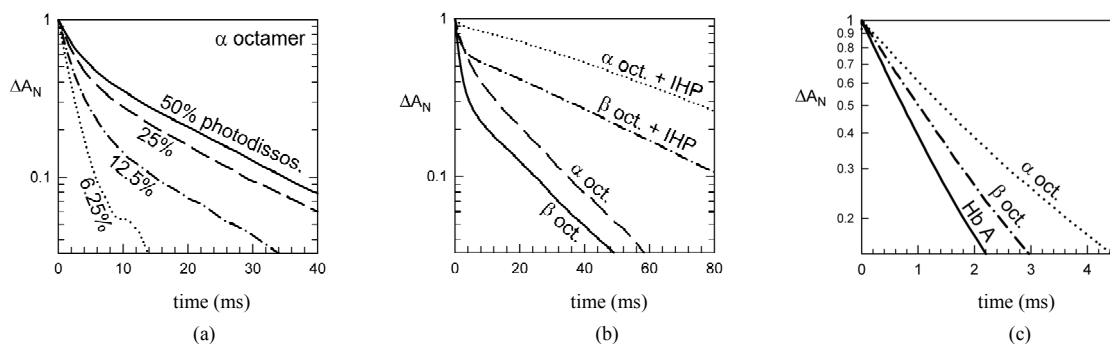
Figure 2. Kinetics of recombination of CO to Hb octamers at 37°C. (a) Kinetics at different fraction of photo-dissociation of the α octamers. Curves are normalized to better show the decrease in the fraction of slow phase, at lower levels of dissociation. At sufficiently low laser energies, the main photoproduct is triply liganded Hb (considering tetramers) which remains in the rapid R-state conformation; (b) IHP favors the fraction of the slow recombination, characteristic of the T-state form. The α octamer shows more of the slow phase, relative to the β analogue (or control Hb tetramers); (c) Kinetics at low photodissociation levels, to isolate the CO recombination to the R-state form, indicate a moderate change in rate for the octamers relative to tetrameric HbA. This difference disappears upon addition of a reducing agent to break the S-S bonds to recover the tetramer form. Note that the tetrameric form of the mutants could within 30 min after addition of 10 mM of DTT. The tetrameric forms of rHb (αAsn78Cys) and rHb (βGly83Cys) show rates similar to HbA, so the differences in rate for the octamers are due to an octameric constraint.

the α, β octamers, and HbA, respectively. These results show that both α and β octamers have an allosteric behavior, with the α octamer shifting more completely to the T-state conformation.

In the red blood cell, the effector DPG promotes the T-state form of Hb. IHP is an analogue of DPG that displays a larger shift in the allosteric equilibrium; for HbA one can observe nearly 100% of the T-state kinetics for samples with 1 mM of IHP at high photodissociation levels (**Figure 2(b)**). In comparison, the α octamer reaches 94% while the β octamer shows only 65% of the T-state phase (**Figure 2(b)**). However, the gain of the amount of T-state is about 35% for both octamers indicating a similar sensitivity to IHP.

3.3. Oxygen Equilibrium Binding Properties

The oxygen-binding properties of α octamer, β octamer

and HbA in the absence and presence of IHP are summarized in **Table 2**. Oxygen affinity (or P_{50}) corresponds to the oxygen partial pressure at 50% saturation of the hemes. The α octamer has an oxygen affinity near to that of HbA while the β octamer has a higher oxygen affinity than that of HbA (e.g., at pH 7.4, P_{50} = 4.7 vs. 8.6 mmHg), and displays a weaker pH dependence. All octamers show a cooperativity of oxygen binding, but there is a decrease in the Hill coefficient relative to the control HbA. The Hill coefficient for the rHbs is slightly lower than that of HbA over the entire range of pH.

3.4. Stability of the Octamers

To investigate the stability of the octameric Hbs, the concentration dependence of the α octamer was studied by SEC on Superose^{TM} 12 HR 10/300 GL column. For the control HbA, one observes a shift of the eluted peak

Table 2. Oxygen Equilibrium parameters of αAsn78Cys and βGly83Cys octamers.

Hb sample	pH	P_{50} (mmHg)	n_{50}	$\Delta(\log P_{50}) / \Delta(pH)$	P_{50} (mmHg)	n_{50}	$\Delta(\log P_{50}) / \Delta(pH)$
			without IHP			with IHP	
HbA	6.5	21.5	2.8	0.45	77.3	1.9	0.71
	7.0	14.9	2.9		45.7	2.1	
	7.4	8.6	3.0		23.8	2.7	
	8.3	3.4	2.9		4.4	3.0	
α octamer	6.5	22.7	2.4	0.35	48.4	1.9	0.54
	7.0	15.0	2.7		40.1	1.7	
	7.4	10.0	2.7		24.2	1.5	
	8.3	5.3	2.6		5.5	2.0	
β octamer	6.5	8.8	2.8	0.27	19.7	1.7	0.46
	7.0	6.5	2.8		12.4	1.2	
	7.4	4.7	2.8		6.2	1.0	
	8.3	2.9	2.9		3.0	1.8	

Samples were in 0.1 M sodium phosphate buffer at 29°C.

with decreasing concentration from the tetrameric to dimeric form. In contrast, irrespective of the applied concentration (from 150 to 6 μM), the α octamer eluted at the same volume (Ve = 11.5 ± 0.01 ml) corresponding to a molecular complex formed by 2 tetramers (results not shown). The width at half height remained small and constant (553 ± 4 μl), indicating a high stability of the α octamer.

Secondly, we studied the stability of the α octamer in the presence of potential reducing agents contained in fresh plasma. The α octamer was incubated in fresh human plasma during 24 h; unlike HbA which forms dimers, the peak does not shift to a higher elution volume (results not shown). These results show that the α octamer remains in its octameric form in fresh plasma, as previously reported for the β octamer. We only observed a slight decrease of the amplitude of the peak at 415 nm, suggesting some heme oxidation.

3.5. Interaction with Human Haptoglobin 1-1

In blood plasma, Hp rapidly binds $\alpha\beta$ dimers to form the Hp$(\alpha\beta)_2$ complex [9], following the reaction scheme: $(\alpha_2\beta_2)$ + Hp $\leftrightarrow$ 2$(\alpha\beta)$ + Hp $\rightarrow$ Hp$(\alpha\beta)_2$. Thus, after a 15 min incubation of HbA with Hp at room temperature, the SEC profile shows the presence of a single peak (Ve = 9.85 ml) corresponding to the elution volume of the Hp$(\alpha\beta)_2$ complex (results not shown) [17]. When the same experiment was performed with the β octamer, the SEC profile of this mixture shows the presence of two species corresponding to free Hp1-1(Ve = 10.3 ml) and free β octamer (Ve = 11.6 ml), indicating that the β octamers do not react with Hp after 15 min of incubation (**Figure 3(a)**, red profile) [17]. For the α octamer (**Figure 3(b)**, pink profile) there was about 6% of a Hp/α octamer

complex (Ve = 8.5 ml), in addition to the main species corresponding to free Hp (Ve = 10.3 ml) and free α octamer (Ve = 11.6 ml).

The octamer/Hp interaction was then studied for longer incubation times; the different molecular species were analyzed at various times by SEC and DLS. While DCL-Hb does not react with Hp after a 24 h incubation, the classical Hp$(\alpha\beta)_2$ complex is stable with a size of 14.0 nm; about 7% of the β octamer has reacted with Hp (**Figure 3(a)**, blue profile) to form the Hp/β octamer complex with a higher size of 15.5 nm.

The reaction of the αAsn78Cys octamer and Hp during gave the most complex results (**Figure 3(b)**), with nearly all the α octamers forming a complex with Hp within 24 h. At different times of incubation, the protein populations were analyzed by SEC; we also measured the size of the different purified complexes by DLS (**Table 3**). A complex was observed for the Hp/α octamer with a similar size to that of the reference Hp$(\alpha\beta)_2$, but as a transient species after only 15 min. For longer times a larger complex was formed, approaching a size of about 60 nm. We thus denote the initial (15 min) transient species as the low molecular weight complex (LMW complex), and the final high molecular weight form (at longer incubation times) as the HMW complex. After a 15-min incubation, the Hp/α octamer (LMW) complex had a size similar to that observed for a fraction of the β octamer after 24 h incubation (**Figure 3(b)** pink profile, **Table 3**). After 2 h of incubation a higher size complex appeared and became the major species after 4 h. After 24 h of incubation nearly all species present in solution has reacted to form a HMW complex with a size of about 56.5 nm. It is important to note that the solution after 24 h of incubation is still perfectly clear and there is no presence of precipitate.
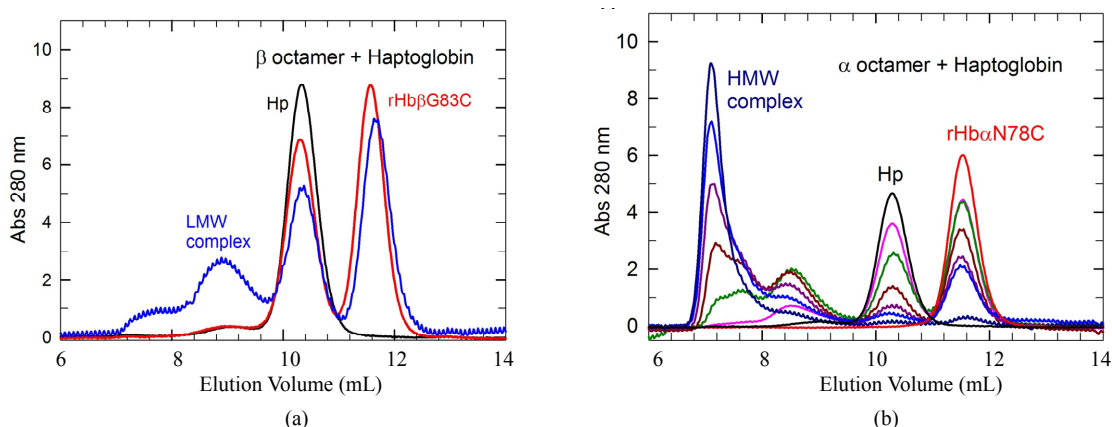
Figure 3. SEC profiles of the β octamer (a) or the α octamer (b) after incubation with Haptoglobin (Hp) versus time. The reactions with Hp were made at 25°C in PBS. At different times, the different species were analyzed on a Superose™ 12 HR 10/300GL column with a flow rate of 0.4 ml/min. For HbA, the initial tetramer peak (at 13 ml) disappears and a new peak at a higher MW (at 9.5 ml) appears, corresponding to the Hp/HbA complex after a 15 min incubation (results not shown). For the β octamers (A), the red and blue profiles represent the different species after an incubation with Hp of 15 min and 24 h, respectively. For the incubation of α octamers with Hp versus time (b), the profiles of different species (decreasing peaks at 10.3 and 11.5 ml; increasing band at 7 ml) were obtained after 15 min (pink), 1 h (green), 2 h (dark red), 4 h (dark pink), 8 h (blue) and 24 h (dark blue).

Table 3. Size of the different purified Hp/Hb complexes obtained by dynamic light scattering for αAsn78Cys octamers, βGly83Cys octamers and HbA.

	Size (nm)	SD
DCL-Hb	6.1	0.3
β octamer	8.1	0.5
α octamer	8.1	0.1
Hp	11.1	0.8
Hp$(\alpha\beta)_2$[a]	14.0	1.3
LMW Hp/α octamer[b]	15.5	1.9
HMW Hp/α octamer[c] 30 µM	56.5	2.6
HMW Hp/α octamer[c] 60 µM	61.4	3.9
HMW Hp/α octamer[d] + DTT	13.1	0.3

The measurements were made after purification of the different molecular species by SEC on Superose™ 12 HR 10/300GL column at 25°C in PBS with a flow rate of 0.4 ml/min. [a]For the reference HbA, the size of the Hp$(\alpha\beta)_2$ complex was the same after a 15 min or 24 h incubation with Hp; [b]The low molecular weight (LMW) form is the initial Hp/α octamer complex, obtained after 15 minutes of contact with Hp. For the Hp/β octamer, a similar size of the Hp/β octamer complex was observed, but only after a 24 h incubation; [c]The complex of Hp/α octamer reaches a final size of about 60 nm (the HMW form) after 10 h; [d]After 24 hours, the HMW form was then reacted with DTT to break the disulfide bonds, which resulted in a return to the size of the reference complex.

The kinetics of the formation of the Hp/α octamer complex was directly studied by dynamic light scattering at 30 µM and 60 µM of each reactant (Hp and α octamer) (**Figure 4**). For the first 2 h, the DLS results consisted of a mixture of sizes for the reactants and initial complex (which are better resolved by the SEC profiles). The overall complex then grows in size to about 60 nm until depletion (after 10 h in our experimental conditions) of free Hp and α octamer reactants. For initial reactants concentrations of 30 and 60 µM, the rate of complex formation was similar, and there was only a small increase in final size (56.5 versus 61.4 nm) at the higher concentration. After 2 h, the LMW transient (at 15.5 nm) decreases in population versus time, representing about 4% of the total after depletion of the Hp and α octamer reactants, as shown in the SEC profile (**Figure 3(b)**). Addition of dithiothreitol (DTT, which breaks the S-S bonds) to the HMW (60 nm) complex leads to a recovery of a lower MW size typical of the Hp/dimer complex.

4. DISCUSSION

The position of disulfide bridges plays a crucial role in the stability and flexibility of proteins. We have previously shown that the presence of a cysteine residue at the β83 position located at the surface of the β-subunit leads

$$(\beta\alpha^{S-S}\alpha\beta)_2 + Hp \overset{1}{\leftrightarrow} 2(\beta\alpha^{S-S}\alpha\beta) + Hp \overset{2}{\to} Hp(\beta\alpha^{S-S}\alpha\beta)_2 \overset{3}{\to} (Hp(\beta\alpha^{S-S}\alpha\beta)_2)_n$$

Octamer   Hemi-Octamer   LMW complex   HMW complex
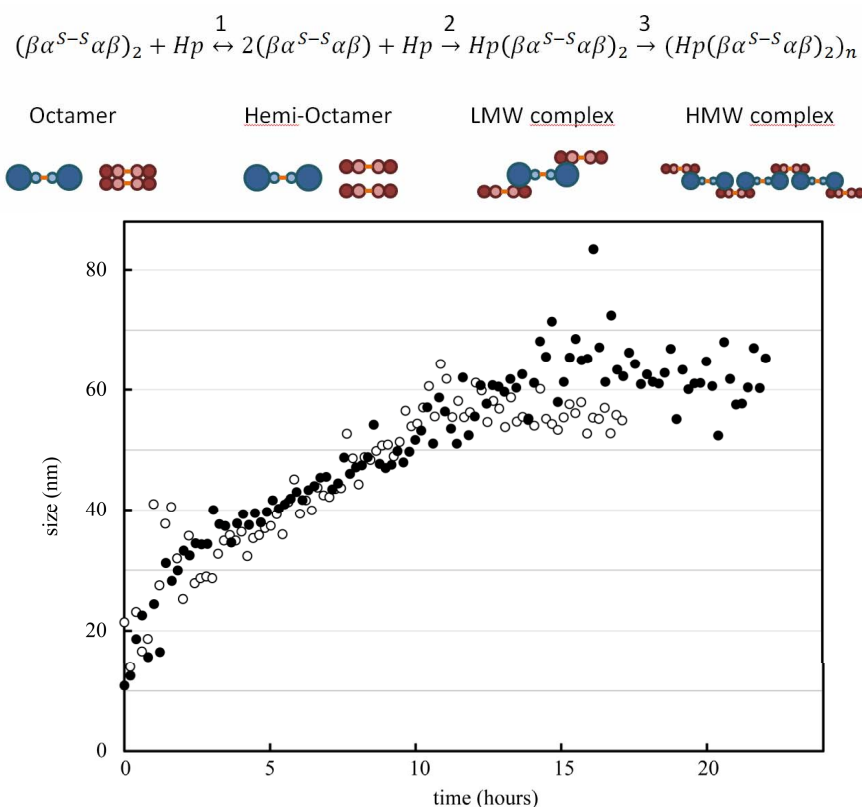
Figure 4. Kinetics of the interaction of Hp with the α octamer. The open circles represent the complex size determined by DLS at 30 μM of each reactant, and the black circles at 60 μM. Note that the size of Hp alone is 11 nm and the Hp/HbA complex is 14 nm. The growth of the complex was independent of the reactant concentration, with a final size near 60 nm. The kinetics were measured at 25°C for samples in PBS. Proposed scheme for the interaction between the α octamer and Hp (top section). The Hp is shown in blue and the α octamer in red, with the α and β-Hb subunits represented in light and dark red, respectively.

to the formation of an octameric Hb which exhibits a high stability in comparison of HbA [8]. Considering its symmetrical position in the EF bend, we replaced α78 Asn by a cysteine residue in order to form a stable oligomer. In the present study, we report the structure and function of rHb (αAsn78Cys) and rHb (βGly83Cys) which introduce a cysteine residue at surface of the α-subunit and β-subunit, respectively. The crystallographic results show clearly that the two rHbs are present in the octameric structure (**Figure 1**).

The function of these octamers as oxygen carriers requires the opposing conditions of maintaining the cysteines in the oxidized state, while keeping the iron atom in the reduced state for oxygen binding. It is thus important to determine whether the response of the octamers in human plasma, where they will be exposed to both oxygen and weak reducing agents, as well as Hp. The present experiments were designed to test the stability and functional properties of the octameric rHbs. The cysteine residues introduced at the surface of the protein were apparently capable of forming the critical S-S bond, but

it was not clear *a priori* as to whether this new conformation would hinder the allosteric transition, and whether the bond could be easily broken by reducing agents.

4.1. Functional Properties of the Octamers

Both the oxygen binding results (**Table 2**) and the flash photolysis kinetics (**Figure 2**) indicate a normal behavior for the octameric rHbs. Indeed as for the native tetramers, the octamers display the two kinetic phases corresponding to the R (rapid) and T (slow) conformations of Hb. The fraction of slow phase decreases as the ligand-dissociation level is decreased (**Figure 2**). To observe this allosteric behavior, the R to T transition must be rapid compared to the CO rebinding. There is thus no apparent resistance of the octamer for the allosteric transition, which must occur simultaneously for both tetramers within the octamer. The α octamer displays a higher fraction of the slow T-like rebinding phase. Note that this is due in part to a better overall photo-dissociation yield. There is generally a geminate recombination on the ns timescale which limits the overall yield for the bimole-

cular phase. Since the α octamer shows a slower R-state, the escape of the photo-dissociated ligand to the solvent may increase. A higher signal amplitude for the α octamer at 4 µs confirms this hypothesis. Comparing the results at similar dissociation levels, as opposed to the same laser level, indicates that the α octamer and HbA have similar allosteric properties, while the β octamer has less T-state at high dissociation levels, consistent with the oxygenation data (**Table 2**).

The oxygen equilibrium binding results also indicate a good allosteric behavior for these octameric systems. In contrast to the β octamer that has a higher oxygen affinity relative to HbA, the α octamer is quite similar in functional properties to the reference HbA. While the overall ligand-binding reactions were similar to the reference tetrameric HbA, two secondary effects can be mentioned. As described in **Figure 2**, the R-state rebinding rate is slower for the octamers relative to the tetramers with the same mutation. This is at first surprising since generally the "relaxed" R-state is little influenced by different mutations or the dissociation to dimers. Reducing the cysteines with DTT (to dissociate the octamers into tetramers) leads to the normal R-state rate, indicating that the octameric form, rather than the mutation, is the cause of the perturbation of the R-state. A similar effect was observed for the fraction of T-like kinetics. While there is a significant difference of the percentage of T-state for the octameric forms, experiments for samples with DTT reveal that the $\alpha(N78C)_2\beta_2$ and $\alpha_2\beta(G83C)_2$ tetramers display about the same amount of the slow T-state kinetics.

The structural studies display the two disulfide bonds per tetramer. A single bond would not be sufficient to explain the stability, since there could be a loss of dimers from each tetramer. With both disulfide bonds, one tetramer could dissociate to dimers, but the octamer would still be held together by the other tetramer. Considering the four β chains within the octamer, a slight intermolecular asymmetry was observed. While the individual subunits maintain the globin form, the Fe-Fe distances were not equivalent, indicating that the geometry of the disulfide bonds differs between the various octamers. Based on the known structures of the tetramer, the distance between the two disulfide bonds can be estimated. They are different for the R and T structures, implying that the two tetramers within the octamer must make the allosteric transition together. Two bonds would also explain the enhanced stability and lack of the dissociation of dimers. This constraint does not seem to hinder the allosteric transition of the tetramers within the octamer. Overall, the octamer can be treated as two functional tetramers, with only a secondary effect of the octameric state on the ligand-binding properties.

The octamer-tetramer reaction is reversible, depending on the redox conditions. For samples under air, octamers form spontaneously, while there is a dissociation into tetramers for samples with reducing agents such as sodium dithionite or DTT. When the octamers were mixed with fresh plasma, there was no shift to the tetrameric form. This was somewhat expected since the free oxygen in the plasma will probably oxidize the cysteines faster any reduction induced dissociation, which requires over 15 minutes.

4.2. Reactivity with Hp

An additional test of protein dissociation is the reaction with Hp, a glycoprotein which specifically captures Hb dimers. Unlike HbA, the octamers did not display a rapid reaction with Hp; however, after 24 h the β octamers show a limited reaction (7%) and the α octamer show a full reaction with the formation of a larger sized complex (**Figure 3**). As the SEC system employed cannot distinguish molecular weights in this high range, we have analyzed the sizes of the complexes by DLS (**Figure 4**). We observed that the Hp/α octamer complex slowly increases in size until the depletion of the free α octamer and Hp. The rate and size of the final HMW complex was nearly independent of the initial reactant concentration; this may reflect the very slow dissociation rate of the α octamer into $\beta\alpha$-$\alpha\beta$, as the association with Hp seems to be fast, at least with HbA. The dissociation of α octamers is probably the rate-limiting for the reaction with Hp. The reaction between the α octamer and Hp can be schematized as shown in **Figure 4**; with a final size of about 60 nm, the geometry is probably not a linear polymer, but perhaps steric constraints induce the system to refold on itself in a cyclic structure involving less than 10 Hp molecules. The addition of DTT leads to the disappearance of the HMW in favor of the reference complex Hp($\alpha\beta$)$_2$. The interpretation is not easy because Hp (1-1) or HLLH contain several cysteines or cystines [12]. Indeed, there are two intra disulfide bridges in the H chains and one in the L chains, in addition to one disulfide bridge between the two L chains and one between the H and L chains [30].

4.3. Conclusion

In conclusion, this study shows that the introduction of a cysteine residue at the surface of the α or β subunit leads to a stable octameric structure whose interaction with Hp are different. Indeed the β octamers did not form a high MW complex with Hp; the reaction could simply be slower, or the orientation of the subunits could play a role and may thus be a probe of the Hp-Hb interaction. The crystallographic structure provides direct evidence for two disulfide bonds per octamer.

5. ACKNOWLEDGEMENTS

REFERENCES

[1] Dickerson, R.E. and Geis, I. (1983) Hemoglobin: Structure, function, evolution, and pathology. The Benjamin/ Cummings Publishing Company, Menlo Park, CA.

[2] Sloan, E.P., Koenigsberg, M., Gens, D., Cipolle, M., Runge, J., Mallory, M.N. and Rodman, G. Jr. (1999) Di-aspirin cross-linked hemoglobin (DCLHb) in the treatment of severe traumatic hemorrhagic shock, a randomized controlled efficacy trial. *Journal of the American Medical Association* (*JAMA*), **282**, 1857-1864. doi:10.1001/jama.282.19.1857

[3] Baudin-Creuza, V., Chauvierre, C., Domingues, E., Kiger, L., Leclerc, L., Vasseur, C., Célier C. and Marden, M.C. (2008) Octamers and nanoparticles as hemoglobin based blood substitutes. *Biochimica et Biophysica Acta*, **1784**, 1448-1453.

[4] Fronticelli, C., Arosio, D., Bobofchak, K.M. and Vasquez, G.B. (2001) Molecular engineering of a polymer of tetrameric hemoglobins. *Proteins*, **44**, 212-222. doi:10.1002/prot.1086

[5] Chauvierre, C., Manchanda, R., Labarre, D., Vauthier, C., Marden, M.C. and Leclerc, L. (2010) Artificial oxygen carrier based on polysaccharides-poly(alkylcyanoacrylates) nanoparticle templates. *Biomaterials*, **31**, 6069-6074. doi:10.1016/j.biomaterials.2010.04.039

[6] Patrinos, G.P., Giardine, B., Riemer, C., Miller, W., Chui, D.H., Anagnou, N.P., Wajcman, H. and Hardison, R.C. (2004) Improvements in the HbVar database of human hemoglobin variants and thalassemia mutations for population and sequence variation studies. *Nucleic Acids Research*, **32**, D537-541. doi:10.1093/nar/gkh006 http://globin.cse.psu.edu/globin/hbvar/

[7] Blackwell, R.Q., Liu, C.S. and Wang, C.L. (1971) Hemoglobin Ta-Li, 83 Gly leads to Cys. *Biochimica et Biophysica Acta*, **243**, 467-474.

[8] Fablet, C., Marden, M.C., Green, B.N., Ho, C., Pagnier, J. and Baudin-Creuza, V. (2003) Stable octameric structure of recombinant hemoglobin alpha(2)beta(2)83 Gly→Cys. *Protein Science*, **12**, 690-695. doi:10.1110/ps.0234403

[9] Nagel, R.L. and Gibson Q.H. (1971) The binding of hemoglobin to haptoglobin and its relation to subunit dissociation of hemoglobin. *Journal of Biological Chemistry*, **246**, 69-73.

[10] Kristiansen, M., Graversen, J.H., Jacobsen, C., Sonne, O., Hoffman, H.J., Law, S.K. and Moestrup, S.K. (2001) Identification of the haemoglobin scavenger receptor. *Nature*, **409**, 198-201. doi:10.1038/35051594

[11] Møller, H.J., Peterslund, N.A., Graversen, J.H. and Moestrup, S.K. (2002) Identification of the hemoglobin scavenger receptor/CD163 as a natural soluble protein in plasma. *Blood*, **99**, 378-380. doi:10.1182/blood.V99.1.378

[12] Wejman, J.C., Hovsepian, D., Wall, J.S., Hainfeld, J.F. and Greer, J. (1984) Structure and assembly of haptoglobin polymers by electron microscopy. *Journal of Molecular Biology*, **174**, 343-368. doi:10.1016/0022-2836(84)90342-5

[13] Shen, T.J., Ho, N.T., Simplaceanu, V., Zou, M., Green, B.N., Tam, M.F. and Ho, C. (1993) Production of unmodified human adult hemoglobin in *Escherichia coli*. *Proceedings of the National Academy of Sciences USA*, **90**, 8108-8112. doi:10.1073/pnas.90.17.8108

[14] Shen, T.J., Ho, N.T., Zou, M., Sun, D.P., Cottam, P.F., Simplaceanu, V., Tam, M.F., Bell, D.A. and Ho, C. (1997) Production of human normal adult and fetal hemoglobins in *Escherichia coli*. *Protein Engineering*, **10**, 1085-1097. doi:10.1093/protein/10.9.1085

[15] Marden, M.C., Kister, J., Bohn, B. and Poyart, C. (1988) T-state hemoglobin with four ligands bound. *Biochemistry*, **27**, 1659-1664. doi:10.1021/bi00405a041

[16] Uzan, J., Dewilde, S., Burmester, T., Hankeln, T., Moens, L., Hamdane, D., Marden, M.C. and Kiger, L. (2004) Neuroglobin and other hexacoordinated hemoglobins show a weak temperature dependence of oxygen binding. *Biophysical Journal*, **87**, 1196-1204. doi:10.1529/biophysj.104.042168

[17] Vasseur-Godbillon, C., Sahu, S.C., Domingues, E., Fablet, C., Giovannelli, J.L., Tam, T.C., Ho, N.T., Ho, C., Marden, M.C. and Baudin-Creuza, V. (2006) Recombinant hemoglobin betaG83C-F41Y. *FEBS Journal*, **273**, 230-241. doi:10.1111/j.1742-4658.2005.05063.x

[18] Pflugrath, J.W. (1999) The finer things in X-ray diffraction data collection. *Acta Crystallographica Section D*: *Biological Crystallography*, **55**, 1718-1725. doi:10.1107/S090744499900935X

[19] Otwinowski, Z. and Minor, W. (1997) Processing of X-ray Diffraction Data Collected in Oscillation Method, Macromolecular Crystallography Part A. *Methods Enzymology*, **276**, 307-326. doi:10.1016/S0076-6879(97)76066-X

[20] Adams, P.D., Grosse-Kunstleve, R.W., Hung, L.W., Ioerger, T.R., McCoy, A.J., Moriarty, N.W., Read, R.J., Sacchettini, J.C., Sauter, N.K. and Terwilliger, T.C. (2002) PHENIX, building new software for automated crystallographic structure determination. *Acta Crystallographica Section D*: *Biological Crystallography*, **58**, 1948-1954. doi:10.1107/S0907444902016657

[21] Otwinowski, Z. and Minor, W. (1993) DENZO. A film processing program for macromolecular crystallography. Yale University, New Haven.

[22] Silva, M.M., Rogers, P.H. and Arnone, A. (1992) A third quaternary structure of human hemoglobin A at 1.7-A resolution. *Journal of Biological Chemistry*, **267**, 17248-17256.

[23] McCoy, A.J., Grosse-Kunstleve, R.W., Storoni, L.C. and Read, R.J. (2005) Likelihood-enhanced fast translation functions. *Acta Crystallographica Section D*: *Biological Crystallography*, **61**, 458-464. doi:10.1107/S0907444905001617

[24] Winn, M.D., Murshudov, G.N. and Papiz, M.Z. (2003) Macromolecular TLS refinement in REFMAC at moderate resolutions. *Methods Enzymology*, **374**, 300-321. doi:10.1016/S0076-6879(03)74014-2

[25] Brunger, A.T. (1992) Free R value, a novel statistical quantity for assessing the accuracy of crystal structures. *Nature*, **355**, 472-475. doi:10.1038/355472a0

[26] Emsley, P. and Cowtan, K. (2004) Coot, model-building tools for molecular graphics. *Acta Crystallographica Section D*: *Biological Crystallography*, **60**, 2126-2132. doi:10.1107/S0907444904019158

[27] Vaguine, A.A., Richelle, J. and Wodak, S.J. (1999) SFCHECK, a unified set of procedures for evaluating the quality of macromolecular structure-factor data and their agreement with the atomic model. *Acta Crystallographica Section D*: *Biological Crystallography*, **55**, 191-205. doi:10.1107/S0907444998006684

[28] Laskowski, R.A., MacArthur, M.W., Moss, D.S. and Thornton, J.M. (1993) PROCHECK, a program to check the stereochemical quality of protein structures. *Journal of Applied Crystallography*, **26**, 283-291. doi:10.1107/S0021889892009944

[29] Collaborative Computational Project, Number 4. (1994) The CCP4 suite, programs for protein crystallography. *Acta Crystallographica*, **D50**, 760-763. doi:10.1107/S0907444994003112

[30] Nielsen, M.J. and Moestrup, S.K. (2009) Receptor targeting of hemoglobin mediated by the haptoglobins: roles beyond heme scavenging. *Blood*, **114**, 764-771. doi:10.1182/blood-2009-01-198309